Oct 23rd, 12:00 AM

Behaviour of Channel Beams with Unbraced Compression Flanges

J. Rhodes

L. K. Seah

Tenth International Specialty Conference on Cold-formed Steel Structures
St. Louis, Missouri, U.S.A., October 23-24, 1990

BEHAVIOUR OF CHANNEL BEAMS WITH UNBRACED COMPRESSION FLANGES

by

L K Seah[1] and J Rhodes[2]

SYNOPSIS

Lips and other types of edge stiffeners are widely used in thin-walled structures. The most common type of edge stiffener is formed by turning the free edge of the unstiffened flange inwards or outwards to form a lip, which substantially improves the buckling resistance of a member thus leading to greater efficiency. In this paper the structural behaviour and strength of edge stiffened beam sections, subjected to bending such that the unbraced edge stiffeners are in compression, are examined both theoretically and experimentally. An outline of two series of tests on edge stiffened beam sections of various geometries is given. Results of the experimental investigation are compared with the theoretical predictions. The agreement between theory and experiment is reasonably good. Design procedures are proposed based on the effective width concept and the theoretical findings to predict the ultimate strength of such edge stiffened beam sections. Comparisons between the experimental and predicted ultimate moments, based on the proposed design procedures are also presented.

1. INTRODUCTION

Edge stiffened thin-walled sections under uniform compression and moments acting in such a way that the stiffened flange is in compression, have received a great deal of research attention in the past. Notable advances have been made in understanding the post-local buckling behaviour of such sections. The case of lipped Channel beam sections bent in such a way that the lips act as compression flanges, has not received so much attention. When the beam is loaded in such a manner, the tension flange of the beam remains straight and does not displace laterally. The unbraced compressed lips, however, tend to buckle in the lateral direction, accompanied by the out-of-plane bending of the web, as shown figures (1) and (2). This buckling phenomenon is particularly noticeable in relatively short lengths of beam.

The problem was probably first tackled by Douty [1] in 1962 and is briefly illustrated in reference [2]. Douty considered the compression portion of the web and the compression lips as a column supported on an elastic foundation where the elastic support is provided by the remaining portion of the web and the tension flange acting together as an elastic frame.

---

1 Department of Mechanical & Production Engineering, Nanyang Technological Institute, Singapore 2263.

2 Currently Visiting Professor of Nanyang Technological Institute, Singapore.
Department of Mechanics of Materials, University of Strathclyde, Glasgow G1 1XJ.

Douty's method is close to the case when the compression lips buckle into numbers of short waves, which is the behaviour more likely to be observed in a long beam with small lips. However, for such a long beam subjected to bending, the lateral-torsional buckling may well be the governing mode of failure.

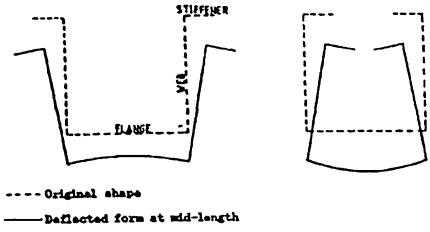

Figure 1

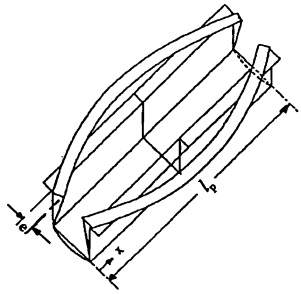

Figure 2

2. OUTLINE OF THEORETICAL ANALYSIS

The analysis is described with reference to the lipped Top-Hat & Channel section shown in figure (3). In the analysis, the beam is treated as a system of plates joined at the edges and acted upon by axial stress systems, due to bending of the beam and lateral distortion of the beam section, as shown in figure (4).

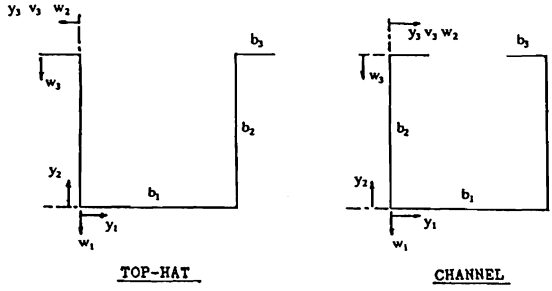

Figure 3

An approximate deflected form is assumed in terms of two unknown arbitrary coefficients. One is the curvature coefficient, 'C', due to bending and the other is the curvature coefficient, 'd', due to the lateral displacement of the lip. The strain energy is then evaluated in terms of these two coefficients. The total change in potential energy of the system is then minimised with respect to the 'd' curvature coefficient, leading to a cubic equation. By specifying the bending curvature, the stresses and moments can be determined and the ultimate moment is determined by assuming that the maximum moment is reached when the maximum compressive membrane stress reaches the material yield stress.

With reference to figures (1) to (3), the assumed deflected form for plates and stiffener are as follows:

For Top-Hat section beam:
The flange; b_1

$$W_1 = \frac{C}{2}(l_p x - x^2) - \frac{d}{2}(l_p x - x^2 - e)\,\mathrm{Sin}\frac{\pi y_1}{b_1} \qquad \ldots(1)$$

For the web; b_2

$$W_2 = \frac{d}{2}(l_p x - x^2 - e)\frac{\pi y_2}{b_1} \qquad \ldots(2)$$

For the stiffener; b_3

$$W_3 = \frac{c}{2}(l_p x - x^2) + \frac{d}{2}\frac{\pi y_3}{b_1}(l_p x - x^2 - e) \qquad \ldots(3)$$

$$V_3 = \frac{d}{2}\frac{\pi b_2}{b_1}(l_p x - x^2 - e) \qquad \ldots(4)$$

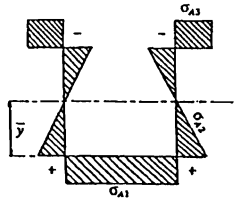

A) STRESSES DUE TO BENDING

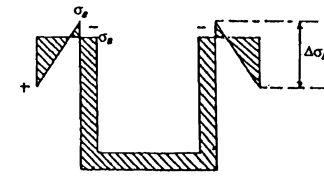

B) STRESSES DUE TO LATERAL-
DISPLACEMENT OF THE LIPS

Figure 4

In the above equations, 'e' represents the cross sectional deflection at the ends of the beam as shown in figure 2. Preliminary analysis shows that such deflection must be included to accurately predict the behaviour. Since the beam is subjected to pure moment, it has only normal stresses with no shearing stresses set up in it. The compatability and moment equilibrium about the web-flange junctions, the lip-web junctions and the free edge are satisfied.

Referring to figure (4), summing the stresses and including the axial shortening due to the lateral displacement of the lips, the stresses on the flange can be written as:

$$\sigma_1 = E\left[c\bar{y} - d\frac{\pi b_2}{b_1}\frac{b_3^2}{A_T}\right] + \frac{E}{2l_p}\int_0^{l_p}\left(\frac{\partial W_1}{\partial x}\right)^2 dx \qquad \ldots(5)$$

The stresses on the web:

$$\sigma_2 = E\left[C(\bar{y} - y_2) - d\frac{\pi b_2}{b_1}\frac{b_3^2}{A_T}\right] + \frac{E}{2l_p}\int_0^{l_p}\left(\frac{\partial W_2}{\partial x}\right)^2 dx \qquad \ldots(6)$$

The stresses on the lip;

$$\sigma_3 = E\left[C(\bar{y}-b_2) - d\frac{\pi b_2}{b_1}\left(\frac{b_3^2}{A_T}-y_3\right)\right] + \frac{E}{2l_p}\int_0^{l_p}\left(\frac{\partial W_3}{\partial x}\right)^2 dx + \frac{E}{2l_p}\int_0^{l_p}\left(\frac{\partial V_3}{\partial x}\right)^2 dx \qquad \ldots(7)$$

where $\bar{y}$ is the distance of the neutral axis to the middle surface of the tension flange before any lateral displacement occurs. A_T is the cross-section of the beam per unit thickness. As the lips buckle separately, the section will open up and these will cause a change in the neutral axis position. If the neutral axis is assumed to remain at the initial position, there will be axial forces set up in the plate system. These axial forces can be determined as follows:

$$\Sigma F = t\int_0^{b_1}\sigma_1 dy_1 + 2t\int_0^{b_2}\sigma_2 dy_2 + 2t\int_0^{b_3}\sigma_3 dy_3 \qquad \ldots(8)$$

In order to satisfy the equilibrium condition, an equal but opposite force is introduced into equations (5), (6) and (7).

The total bending energy, V_{BT} for the flange, webs and lips is:

$$V_{BT} = V_{B1} + 2V_{B2} + 2V_{B3} \qquad \ldots(9)$$

Where 'V_{Bi}' is bending energy of individual plates:

$$V_{Bi} = \frac{D}{2}\int_0^{l_p}\int_0^{b}\left\{\left[\frac{\partial^2 w_i}{\partial x^2}+\frac{\partial^2 w_i}{\partial y^2}\right]^2 + 2(1-\nu)\left[\left(\frac{\partial^2 w_i}{\partial x \partial y}\right)^2 - \frac{\partial^2 w_i}{\partial x^2}\frac{\partial^2 w_i}{\partial y^2}\right]\right\} dx\,dy$$

$\ldots(10)$

i=1, 2 or 3

A minimum value of V_{BT} arises at a particular 'e' value, and can be determined by differentiating the total bending energy 'V_{BT}' with respect to 'e', gives:

$$e = \frac{l_p^2}{6} + 2\upsilon\left(\frac{b_1}{\pi}\right)^2\left(1-\frac{4}{\pi}\frac{C}{d}\right) \qquad \ldots(11)$$

To simplify the analysis, the 'e' value can be taken as:

$$e = \frac{l_p^2}{6} \qquad \ldots(12)$$

If the membrane shear stresses and stresses in the y-direction were neglected, the membrane energy due to deformation of the middle plane of a plate element by forces applied in this plane is:

$$V_M = \frac{1}{2E}\int_v \sigma_x^2 dv \qquad \ldots(13)$$

Applying this equation to a system of plates, the total membrane energy for the whole system of plates can be written as:

$$V_{MT} = \frac{1}{2E}\left\{\int_{v1}\sigma_1^2 dv_1 + 2\int_{v2}\sigma_2^2 dv_2 + 2\int_{v3}\sigma_3^2 dv_3\right\} \qquad \ldots(14)$$

The total potential energy change, $V_T=V_{MT}+V_{BT}$, which is too lengthy to be detailed here can now be minimised respect to the curvature coefficient 'd', which will yield the following cubic expression:

$$d^3J_1+d^2J_2+dJ_3+J_4=0 \qquad ...(15)$$

where:

$$J_1=\frac{l_p^4}{144}B_6$$

$$J_2=\frac{l_p^2}{2}B_8$$

$$J_3=\frac{t^2}{6(1-\upsilon^2)}B_1+2B_4-C\frac{l_p^2}{3}B_7$$

$$J_4=C\left[2B_5-\frac{t^2}{12(1-\upsilon^2)}B_2\right]$$

The numerical constants, 'B_i' are detailed in Appendix I.

Equation (15) can be solved to obtain the 'd' curvature for a specific value of the 'C' curvature. A numerical method known as Muller'S method is used to solve equation (15) for multiple roots, and the minimum, non-zero positive root is used in calculation of the corresponding bending moment. If considering only the linear 'd' terms. The following expression is obtained:

$$d=\frac{C\left[\frac{t^2}{12(1-\upsilon^2)}B_2-2B_5\right]}{\left[\frac{t^2}{6(1-\upsilon^2)}B_1+2B_4\right]} \qquad ...(16)$$

The moments on the beam can be calculated by summation of moments about an axis through the tension flange, giving:

$$M=2b_2t\int_0^{b_3}-\sigma_3dy_3+2t\int_0^{b_2}-\sigma_2y_2dy_2 \qquad ...(17)$$

The theoretical ultimate moment of the lipped beam section is determined based on a simple yield criterion, i.e. when the maximum compressive stress at any point reaches the material yield stress.

Another parameter of particular interest is the centre deflection of the beam. The actual loading during the experiment is four point bending. But, since the distance between the support and loading knife edge is kept small compared to the distance between the two loading knife edge, the centre deflection can then be approximated by assuming that the simply supported beam was under pure moment of such magnitude, i.e.

$$\delta_c=\frac{Cl_s^2}{8} \qquad ...(18)$$

3. THE INITIAL INSTABILITY OF BEAMS WITH SMALL LIPS

When the width of the lips is small, there may be a tendency to buckle into more than one half-wave and it is important to know the moment that causes the onset of this instability. The critical moment in such a case can be determined by setting the "J_3" term in equation (15) equal to zero. The reason is, if the assumed deflected forms used vary sinusoidally instead of parabolically, then the 'J_4' term in equation (15) will become zero for buckling into more than one half-wave and equation (15) becomes:

$$d^2J_1 + dJ_2 + J_3 = 0 \qquad \ldots(19)$$

Note if the number of buckle half-waves is even, then the 'J_2' term in equation (15) will also become zero. At the point of buckling (ie. d=0), J_3=0, this gives the critical curvature 'C_{CR}' as:

$$C_{CR} = \frac{3}{l_p^2 B_7}\left[\frac{t^2}{6(1-\upsilon^2)}B_1 + 2B_4\right] \qquad \ldots(20)$$

The critical curvature in equation (20) has a minimum value with respect to the length. This minimum value can be obtained by differentiating the equation (20) with respect to l_p and equating to zero, yields the following expressions.

for e=0:

$$l_{pmin}^4 = \frac{120}{\pi^4}\left[b_1^4 + \frac{4}{3}\pi^2 b_1(b_2^3 + b_3^3) + \frac{24(1-\upsilon^2)}{t^2}b_1^3 B_4\right] \qquad \ldots(21)$$

for $e = l_p^2/6$:

$$l_{pmin}^4 = \frac{4}{\pi^4\left(\frac{1}{30} + \frac{1}{\bar{e}} - \frac{1}{3\bar{e}}\right)}\left[b_1^4 + \frac{4}{3}\pi^2(b_2^3 + b_3^3) + \frac{24(1-\upsilon^2)}{t^2}b_1^3 B_4\right] \qquad \ldots(22)$$

where: $\bar{e} = l_p^2/e = 6$

Substituting these value of 'l_{pmin}' as 'l_p' into equation (20) gives the minimum critical curvature. A comparison of this critical curvature with those determined by assuming sinusoidal deflected forms, for both c and d curvatures, is shown in figure (5). In this figure, the average critical curvature approximates to the solution for a beam under constant moment obtained from the analysis using a sinusoidal deflected forms agree quite well with the solutions obtained from the analysis using a parabolic deflected form of e=0 case. But if the ends of the lips are allowed to displace laterally ($e = l_p^2/6$ case), a much lower critical curvature is obtained. Therefore, especially for short lengths of beams the ends of the lips must be allowed to displace laterally in the analysis.

Figure (6) shows the comparison of the stress ratio, for varying aspect ratios, between the analysis described in this chapter and the Finite Strip [3] results. Due to the nature of the method used in this analysis, an upper bound solution is expected. Therefore, for the e=0 case, the analysis results are higher than Finite Strip results since the Finite Strip is a more accurate analysis. For $e = l_p^2/6$ case, the Finite Strip result is higher since it didn't consider the 'e' term in the formulation, and this has been shown to be of high importance.

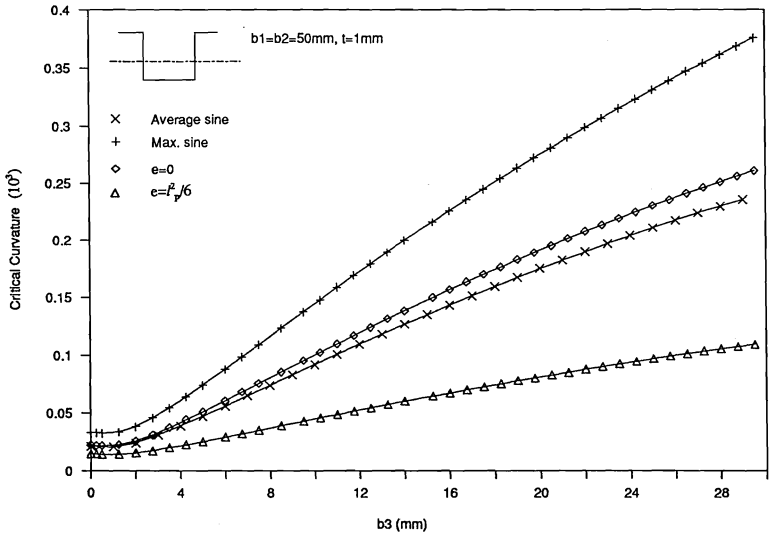

Figure 5

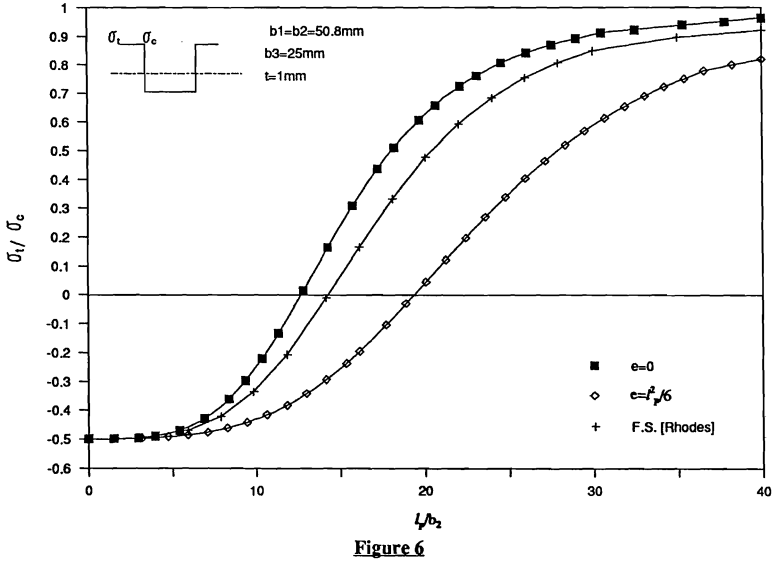

Figure 6

Figure (7) shows the comparison of the critical stress calculated using equation (20), and results obtained from the Finite Strip program developed by Rhodes [3], and from Douty's [1] method which is illustrated in reference [2]. It can be seen from this figure that the Finite Strip results are slightly above the results

of equation (20) for $e = l_p^2/6$ cases, which in fact is an upper bound solution. For the particular dimensions used in this figure, Douty's [1] method suggests that the lips will buckle inelastically at a lip size of about b_3/b_2=0.16, based on an equivalent column analysis. If only elastic buckling is considered, Douty's solutions are close to solutions of equation (20).

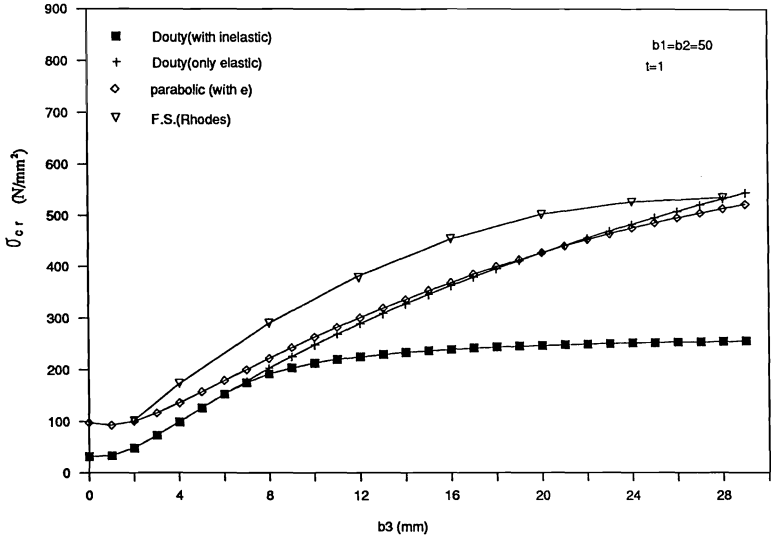

Figure 7

In the actual situation, the single half-wave deflections exist even if the moment is small. This means that at the point of buckling the 'd' curvature due to the single half-wave buckle mode is not equal to zero. Hence, in order to obtain an approximate critical moment for this complex buckling problem, the following procedure is set-up:

i) First, assume d=0 and obtain 'C_{CR}' using equation (20) and equation (22)

ii) Substitute 'C_{CR}' into equation (15), and obtain the corresponding 'd' curvature.

iii) With these 'C_{CR}' and 'd' curvatures, the corresponding critical moment can be approximated using equation (17).

4. EXPERIMENTAL INVESTIGATION

An experimental investigation was carried out in order to obtain information on the behaviour of beams, produced by cold-forming to normal engineering tolerances, under moment action, and to compare the results with those of the theoretical solution. Two series of tests were carried out where the specimens are manufactured from galvanised mild steel sheet.

Spec. No.	t (mm)	L (mm)	b1 (mm)	b2 (mm)	b3 (mm)	σ_y (N/mm^2)
AT1	0.88	915	52.38	51.42	0	289.6
AT2	0.87	915	52	52.24	8.04	289.6
AT3	0.88	915	53.12	52.62	10.77	289.6
AT4	0.87	915	52.7	53.64	13.8	289.6
AT5	0.89	915	53.36	52.42	16.98	289.6
AT6	0.87	915	54.06	52.14	20.36	289.6
AT7	0.87	915	53.08	52.5	23.43	289.6
AT8	0.88	915	54.17	52.45	26.61	289.6
AT9	0.967	915	52.784	51.2	0	307.45
AT10	0.97	915	51.99	51.2	7.34	307.45
AT11	0.97	915	51.6	51.5	10.72	307.45
AT12	0.97	915	51.6	51.65	13.1	307.45
AT13	0.97	915	51.99	50.4	17.07	307.45
AT14	0.97	915	52.39	50.8	20.05	307.45
AT15	0.97	915	52.39	52.19	22.33	292.21
AT16	0.96	915	52.2	51.6	26.89	307.45
AT17	1.136	915	51.594	51.2	0	315.6
AT18	1.14	915	53.18	51.4	7.74	315.6
AT19	1.14	915	52.18	51.45	10.62	315.6
AT20	1.14	915	52.98	50.9	13.89	315.6
AT21	1.14	915	53.18	51.1	16.77	315.6
AT22	1.15	915	51.99	51.89	19.84	315.6
AT23	1.15	915	53.18	51.59	22.82	295.4
AT24	1.15	915	52.39	52.09	26	315.6

TABLE 1 SPECIMEN'S DIMENSIONS (TOP-HAT)

Spec. No.	t (mm)	L (mm)	b1 (mm)	b2 (mm)	b3 (mm)	σ_y (N/mm^2)
AC1	0.81	915	50.93	50.29	0	284.41
AC2	0.81	915	50.66	50.21	0	284.41
AC3	0.81	915	50.69	50.57	6.47	284.41
AC4	0.81	915	50.35	50.30	6.3	284.41
AC5	0.81	915	50.77	50.85	9.59	284.41
AC6	0.81	915	50.55	50.51	9.74	284.41
AC7	0.82	915	51.73	51.66	13.42	277.04
AC8	0.82	915	50.72	50.60	12.74	284.41
AC9	0.98	915	53.76	51.56	0	314.8
AC10	1.04	915	50.67	49.88	0	314.8
AC11	0.97	915	50.83	50.08	6.28	298.96
AC12	1.03	915	50.37	50.25	6.64	314.8
AC13	0.98	915	50.99	50.80	8.94	314.8
AC14	1.03	915	50.55	50.27	10.24	314.8
AC15	1.08	915	50.36	50.33	12.37	314.8
AC16	1.03	915	50.55	50.23	12.59	276.42
AC17	1.13	915	50.72	50.43	0	241.8
AC18	1.14	915	51.04	50.44	0	241.8
AC19	1.15	915	50.26	49.87	6.3	241.8
AC20	1.15	915	50.31	49.10	6.74	241.8
AC21	1.15	915	51.42	50.33	9.59	241.8
AC22	1.15	915	51.05	50.58	9.33	241.8
AC23	1.14	915	51.41	50.99	12.63	273.31
AC24	1.15	915	51.47	51.23	12.84	241.8

TABLE 2 SPECIMEN'S DIMENSIONS (CHANNEL)

The first series of tests consists of 48 beams, of which 24 are outwardly turned lipped Top-Hat sections and 24 are inwardly turned lipped Channel sections. The nominal lip widths varied from 0 to 25mm for the Top-Hat sections. For the Channel sections, the nominal lip widths varied from 0 to 12.7mm. All the 48 beams were 915mm in length, with three nominal thickness of steel sheet; 0.8mm, 1.0mm, and 1.2mm. The nominal widths of the web and flange were both 50mm. The geometry and average centre line dimensions of this series of specimens are given in tables 1 and 2.

The second series of tests consisted of 8 Top-Hat specimens, which were 2m in length initially with a nominal thickness of steel sheet of 0.75mm. The widths of the web and flanges were 50mm and the width of the lips were 15mm. Three out of the eight specimens were cemented with strain gauges, at midlength as shown in figure (8). The main purpose of the strain investigation was to obtain an idea of how the variation of the membrane stress on the lips is affected by the length of the beam. The geometry and average centre line dimensions of this series of specimens are given in table 3

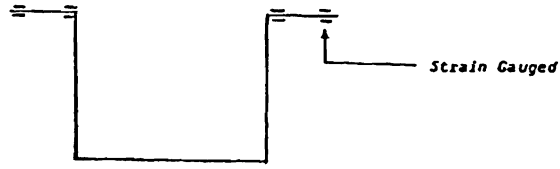

Figure 8

spec. no	t (mm)	b1 (mm)	b2 (mm)	b3 (mm)	l_p at failure (mm)	Mexp (kN.mm)
BT1	0.76	51.24	41.24	14.62	400	284.8
BT2	0.75	47.25	40.25	14.125	600	295.36
BT3	0.75	50.25	39.25	14.125	1600	163.68
BT4	0.76	51.24	40.24	14.62	1600	161.98
BT5	0.76	49.24	41.24	14.62	1600	145.98
BT6	0.75	51.25	40.25	10.625	1600	142.4
BT7	0.76	51.24	40.74	6.62	1600	172.66
BT8	0.75	50.25	39.25	0	1600	72.98

TABLE 3 SPECIMEN'S DIMENSIONS (TEST SERIES 2)

The specimens were tested to failure on a Tinius Olsen Testing Machine with readings of deflections, strains, loads taken during the tests. The test rig is shown diagrammatically in figure (9).

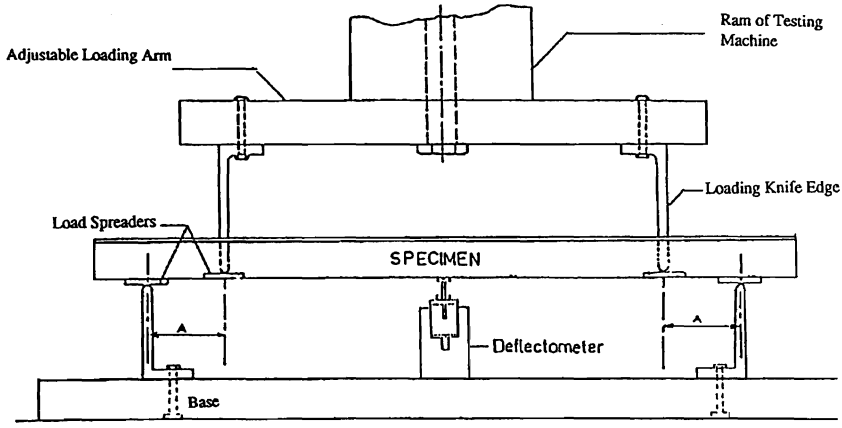

Table of Testing Machine

Figure 9

The two strain gauged specimens namely BT1 & BT2, in test series B were tested in a slightly different way. Initially, the span of these two beams was 2m, the loading was applied to about 1/3 of the predicted failure load and then they were unloaded. The beam length was then cut to 1.8m and loaded again to about 1/3 of the predicted failure load. The process was repeated 6 times, each time the length of the beam being shortened by 200mm. At a final length of 0.8m and 1.0m respectively, the beam was loaded until the collapse occurred.

5. EXPERIMENTAL RESULTS AND OBSERVATIONS

5.1 Test Series A

Typical examples of the buckled shape of the lips for the Top Hat and Channel sections are shown in figures (10), (11) and (12).

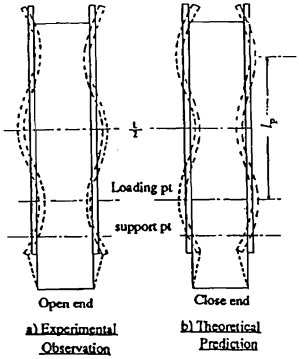

Figure 10

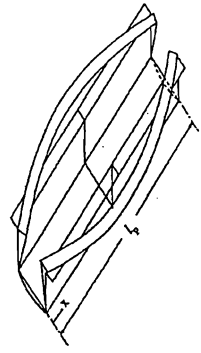

Figure 11

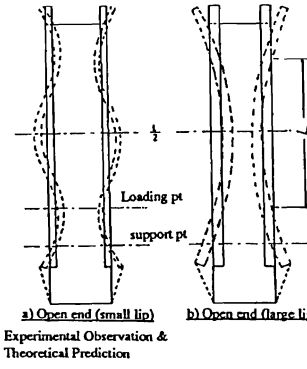

Figure 12

It was observed during experiment that when the lip width is more than or equal to about 12mm, the lips buckled into a single half-wavelength. For the Top Hat section the lips buckled in such a way that the section was opening up at mid-length, as shown in figure (11), and for Channel the section was closing in at mid-length, as shown figure (12b). However when the lip width is smaller than about 12mm the lips of both Top Hat and Channel sections buckled into more than one half-wave length. It was also noticed during experiment that when the lips buckled into more than one half-wave length, the buckling configuration for both Top-Hat and Channel sections is the same (Figures 10a and 12a). This is most probably due to the downward movement of the loading knife edges which forced the lips of the Top-Hat section to buckle into the same configuration as the Channel section. In a further examination of this problem theoretically, using $\mathrm{Sin}\frac{\pi x}{l}$ and $\mathrm{Sin}\frac{3\pi x}{l}$ terms in the deflected forms; equations (1), (2) and (3) become:

For the tension flange;

$$W_1 = \frac{C}{2}(l_p x - x^2) - d\,\mathrm{Sin}\frac{\pi x}{l_p}\mathrm{Sin}\frac{\pi y_1}{b_1} - F\,\mathrm{Sin}\frac{3\pi x}{l_p}\mathrm{Sin}\frac{\pi y_1}{b_1}$$

For the webs;

$$W_2 = d\frac{\pi y_2}{b_1}\mathrm{Sin}\frac{\pi x}{l_p} + F\frac{\pi y_2}{b_1}\mathrm{Sin}\frac{3\pi x}{l_p}$$

For the lips;

$$W_3 = \frac{C}{2}(l_p x - x^2) + d\frac{\pi y_3}{b_1}\mathrm{Sin}\frac{\pi x}{l_p} - F\frac{\pi y_3}{b_1}\mathrm{Sin}\frac{3\pi x}{l_p}$$

Carrying out the same analysis procedures, gives the predictions that for Top-Hat beam section, the minimum potential energy occurs at a buckling configuration in the opposite direction to that which had been observed in the experiment. The observed and predicted buckling configurations are shown in figure (10a&b). However, for the Channel beam section, the predicted buckling configuration and those observed in the experiment is the same (Figure 12a). Therefore, it may be concluded that when the lip width is less than 12mm, the downward movement of the loading knife edges will help the lips of the Channel section to buckle more quickly and fail at a lower moment. For the Top-Hat section however this may not increase the moment carrying capacity.

During the initial test, two of the specimens failed by local crushing of the flange. This type of failure was avoided in the remainder of the tests by providing more substantial load spreaders at the points of loading and support.

5.2 Test Series B

During the experiment, it was observed that for specimens of 2m length, even though the load is applied through the axis of symmetry, the beam failed by the lateral-torsional buckling mode and this is further confirmed by the Finite Strip program developed by Rhodes [3]. This problem is outwith the scope of the present investigation, therefore the results will not be discussed but will be published in a future paper.

6. COMPARISON OF THEORETICAL AND EXPERIMENTAL RESULTS

Figures (13), (14) and (15) shows the comparison of the predicted and experimental stress distribution for specimens AT14, BT1 and BT2 respectively.

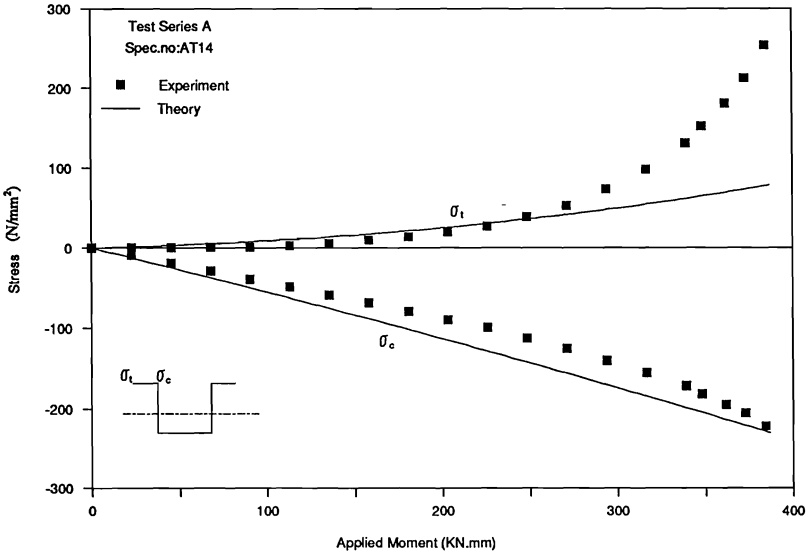

Figure 13

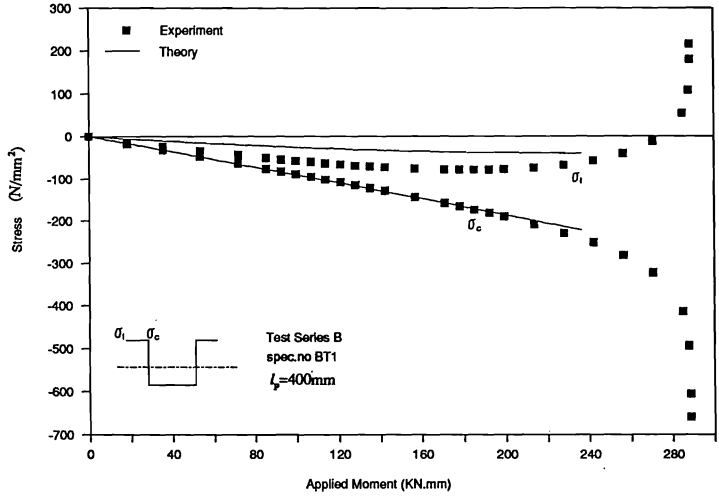

Figure 14

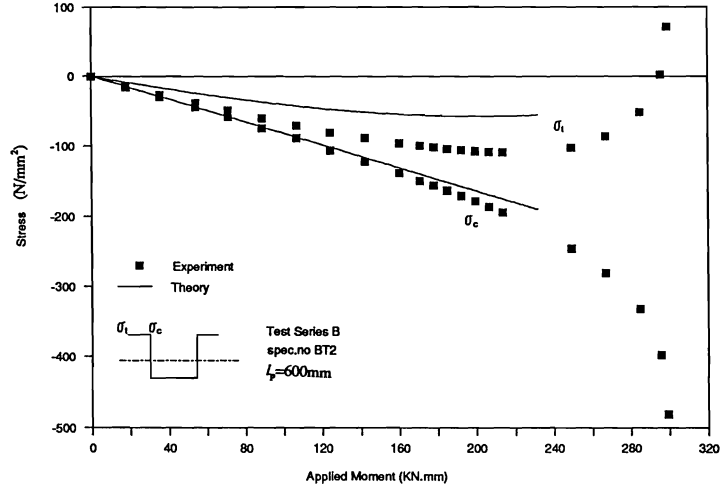

Figure 15

The stresses in figure (13) were plotted until the point at which the loading knife edges obstructed the buckled lips. In these figures, the predicted stresses at the lip-web junction (σ_c) agree quite well with the experimental results up to the point of collapse, but the stresses at the lip free edges only agree in the linear range. However, the prediction of the failure moment was based on compression yield, since yield in tension might not cause collapse of the beam.

Figures (16) to (21), shows the comparison of the theoretical ultimate moments with those obtained experimentally, in non-dimensional form. The theoretical ultimate moments are computed based on the average dimensions of specimens. These figures show a reasonably good agreement between theory and experiment. The maximum discrepancies for Top-Hat sections are within about 26% on the conservative side in all cases. For the Channel sections, the maximum overestimation and underestimation are about 8.4% and 33% respectively.

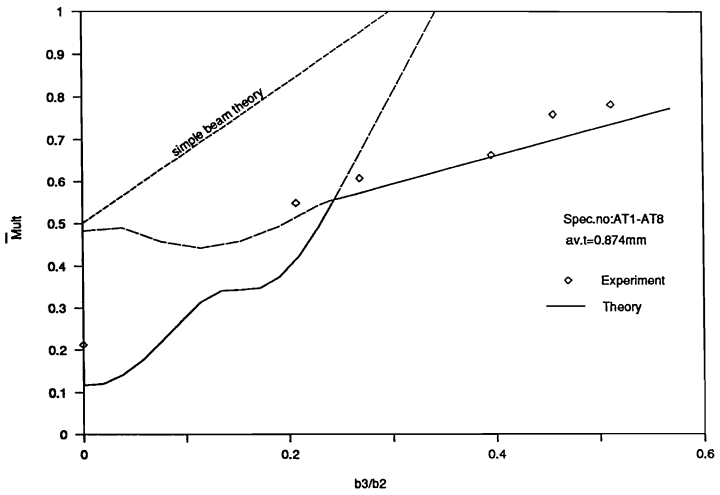

Figure 16

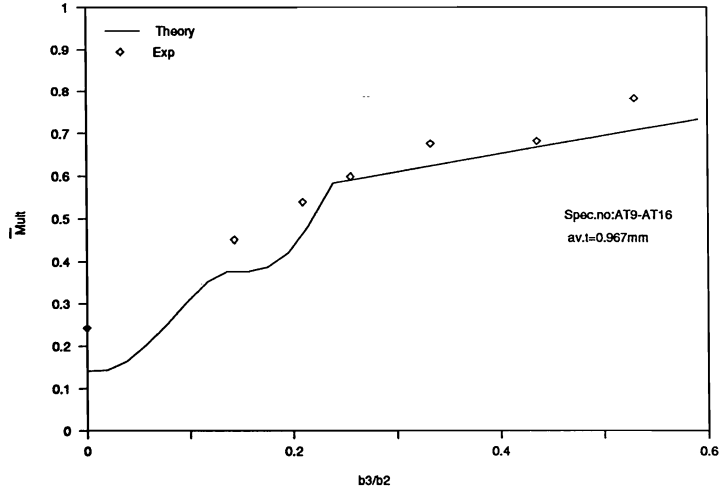

Figure 17

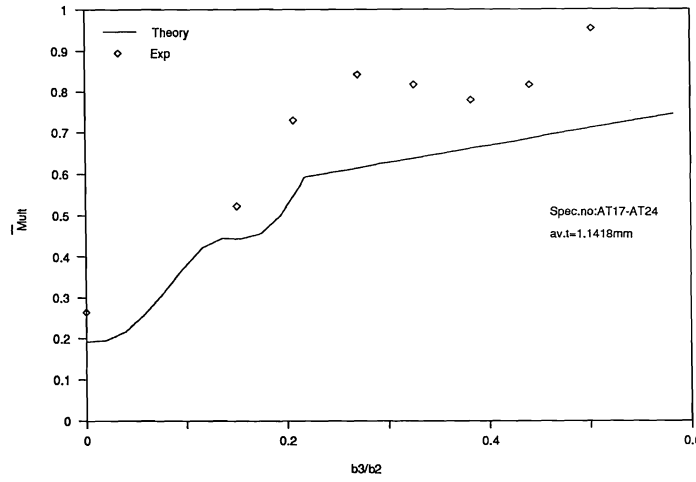

Figure 18

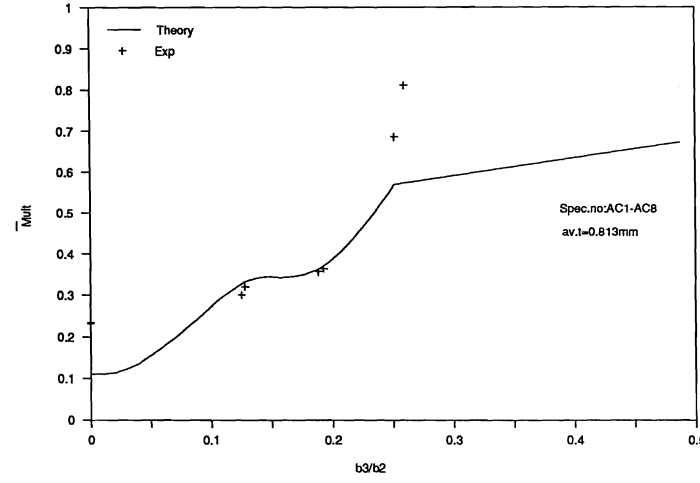

Figure 19

The theoretical curve on these figures consist of two portions. The left side of the curve was drawn based on the criterion that the ultimate moment of the beam is the critical moment. The right side of the curve was drawn based on the assumption that the ultimate moment of the beam is reached when the maximum compressive membrane stress reaches the material yield stress. For design purposes, the cross over point of the theoretical curves may be used as a reference point for the stiffener rigidity requirements. It can be seen that the moment carrying capacity, although still increasing, is not significantly improved by increasing the lip width beyond this reference point. It is noticed that this reference point suggests decreasing lip requirements as the thickness increases.

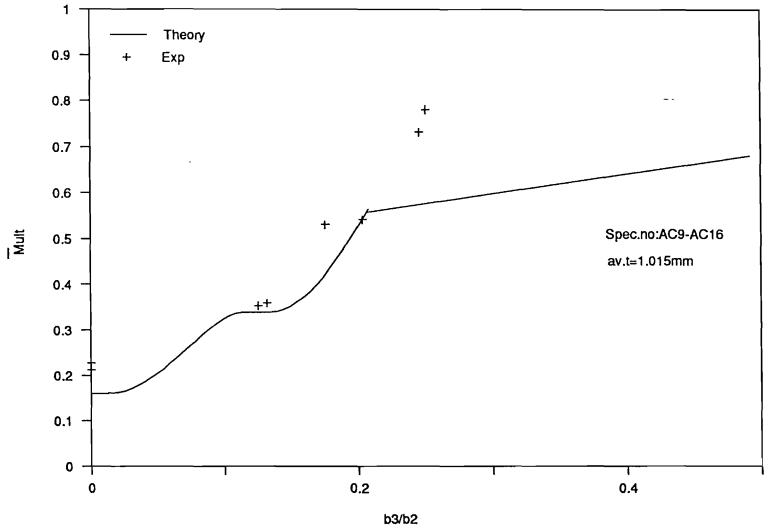

Figure 20

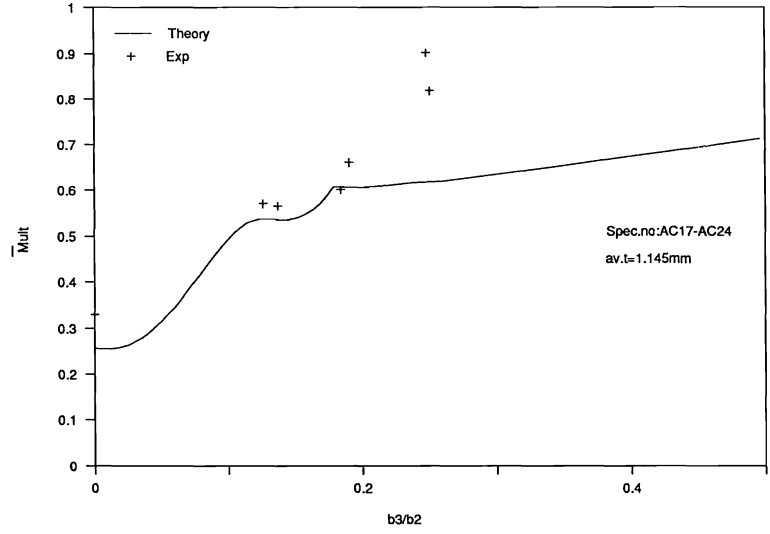

Figure 21

Figure (16), shows also the ultimate moment determined using simple beam theory, which is substantially overestimate compared to the experiment. Also notice that the Channel section beams with lip widths less than 12mm generally carried lower moments than Top-Hat section beams with the same lip widths.

Figure (22), shows that as the length increases, the stress ratio σ_t/σ_c approaches unity. The compression lips tend to buckle more seriously as the length of the beam decreases. The experimental and theoretical results shown follow a similar trend. The theoretical curve in this figure is based on the linear terms only.

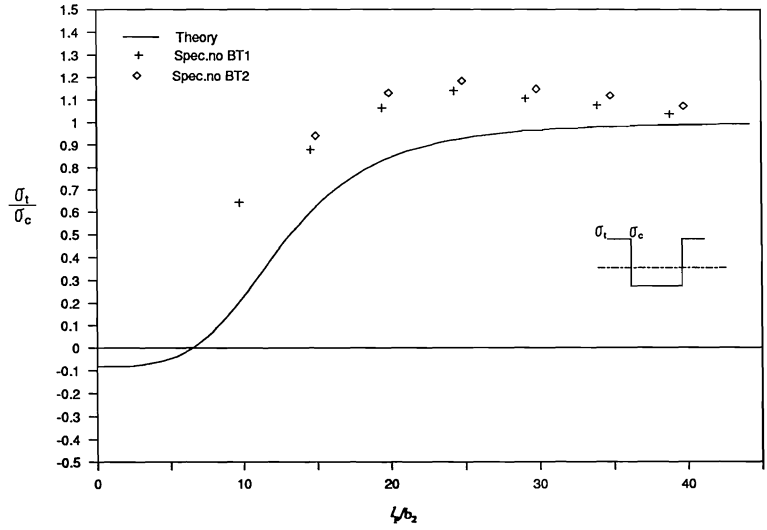

Figure 22

TABLE 4 COMPARISON OF EXPERIMENTAL ULTIMATE MOMENTS WITH THEORETICAL PREDICTIONS (SERIES 2:TOP HAT BEAM)

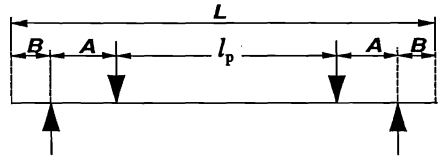

spec. no	t (mm)	l_p (mm)	b3 (mm)	A (mm)	Mexp (kN.mm)	Mth (kN.mm)	Mth/Mexp
BT1	0.76	400	14.62	160	284.8	236.03	0.83
BT2	0.75	600	14.13	160	295.36	231.6	0.784

Figures (23) to (26), show some of the typical moment-deflection curves. Good correlation of the beam's stiffness is obtained between the experimental curves and theoretical predictions. The comparisons for specimens of 2m length are shown in table (4).

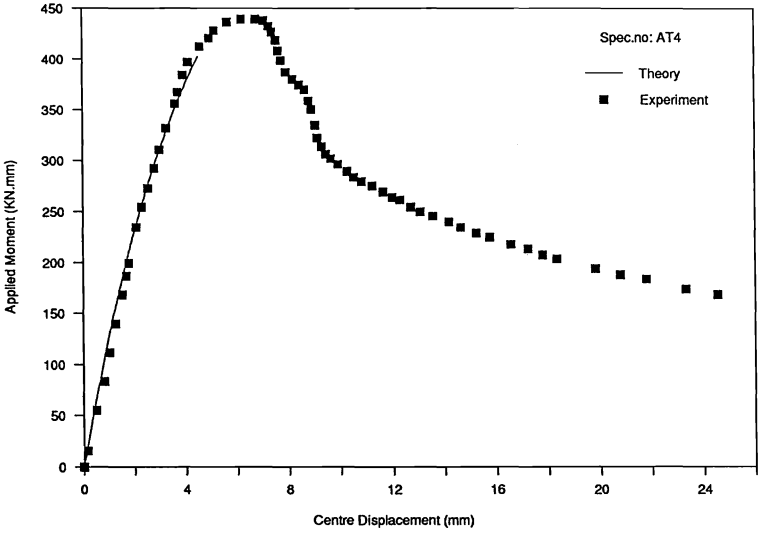

Figure 23

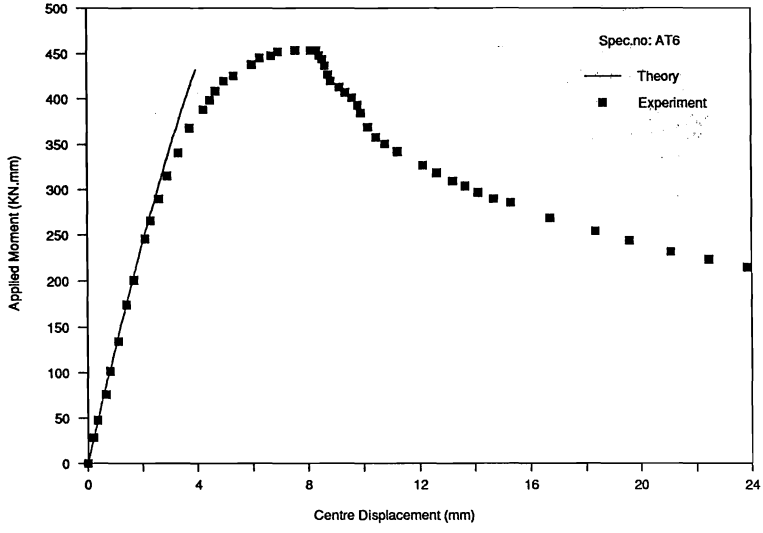

Figure 24

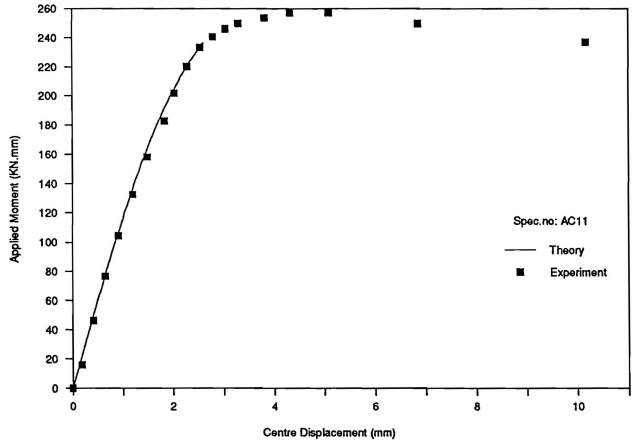

Figure 25

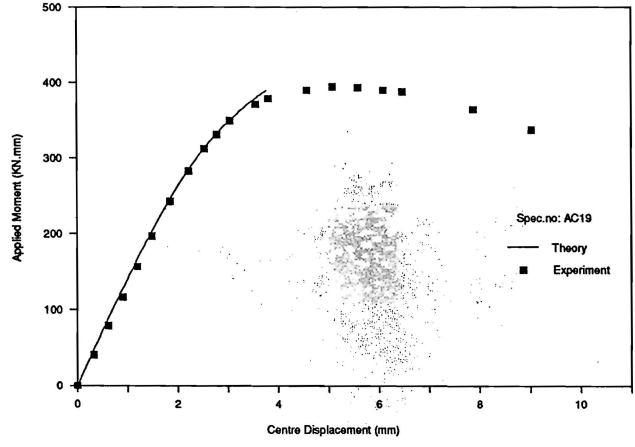

Figure 26

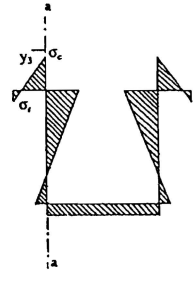

Figure 27

7. FORMULATION OF DESIGN PROCEDURES

Consider the Top-Hat section beam shown in figure (27), with the axial stress system acting upon the section. For an equivalent effective width of the lip, (b_{3eff}) which carries the same load, b_{3eff} must be

$$\frac{b_{3eff}}{b_3}=\frac{1}{2}(1+\sigma_R) \qquad \ldots(23)$$

where

σ_t=stress at the free edge of the lip.

σ_c=Stress at the lip-web junction

$\sigma_R=\frac{\sigma_t}{\sigma_c}$, should be less than or equal to unity.

Using equation (23), the effective compression section modulus (Z_c) can be evaluated, and ultimate moment can be determined.

For design purposes, only the linear terms in the analysis are taken into account. For a practical range of parameters, where L_b is from 0 to 50, R is from 0.25 to 1.5, h_L is from 0.05 to 0.65 and h_t is from 10 to 210. It was found by trial and error that the stress ratio, σ_R expressed as below has the best fit:

$$\sigma_R=-0.5R^n+1.5^{R^s}\left[\frac{L_b^2+L_b}{(10h_L)^m+L_b^2+L_b}\right]^{h_t/R^p} \qquad \ldots(24)$$

where, n=0.25, m=1.25
s=0.24, p=0.75

and σ_R must not be greater than unity.

From the experiment, it was observed that for specimens with (b_3/b_2) ratio of less than about 0.25, the lips will buckle into more than one half-wave length. Since for simple lips the (b/t) ratio is limited to 60, this (b_3/b_2) ratio will be used as an adequacy requirement. For beam sections with (b_3/b_2) ratio of more than 0.25, the effective widths of the lips are calculated using equations (23) and (24). For beam sections with (b_3/b_2) ratio of less than 0.25, the moments are determined as follows:

$$Z_{inad}=Z_u+4(Z_s-Z_u)\frac{b_3}{b_2} \qquad \ldots(25)$$

or, in general, equation (25) can be written as:

$$M_{inad}=M_u+4(M_s-M_u)\frac{b_3}{b_2} \qquad \ldots(26)$$

The ultimate moment of an unstiffened beam sections (M_u) is determined according to B.S. 5950: Part 5, sec 5.2.2.5 [5].

8. COMPARISON OF EXPERIMENTAL AND PREDICTED ULTIMATE MOMENT.

Figures (28) and (29), show the comparison of the experimental ultimate moments with those calculated using simple beam theory with the allowable stress determined according to the Douty's design procedures, without using any factors of safety. These figures shows that Douty's design ultimate moments tend to overestimate the experimental results, accept for small lip width specimens. The comparisons are in better agreement for Channel sections than Top-Hat sections, since the b_3/b_2 ratios of the Channel sections are not more than about 0.25. The maximum overestimation is 51%.

The graphical comparisons of the proposed design procedures are also shown in these figures, with corresponding values shown in table (5). In table (5), the very high overestimation of those thin Channel sections with b_3/b_2 ratio less than 0.2, namely, specimen AC3, AC4, AC5, and AC6, was due to the fact that in these tests the downward movement of the loading knife edges forced the lips to buckle more quickly and fail at a lower load than would otherwise be the case. If these four results are discounted, then the predicted results show very good agreement with the experimental results, overall on the conservative side. The maximum overestimation and underestimation will then be 16% and 25.2% respectively.

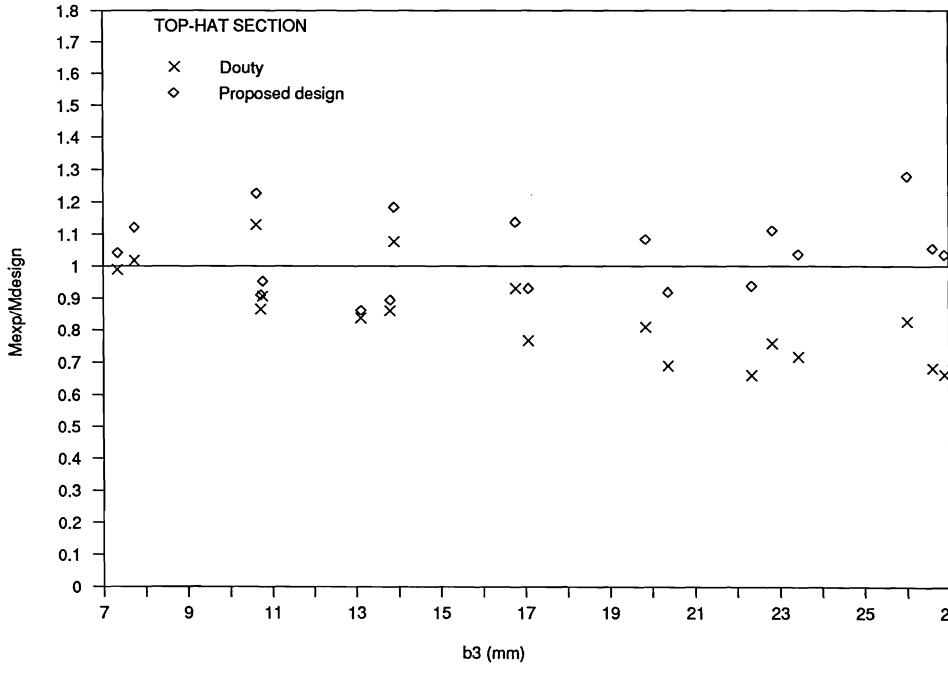

Figure 28

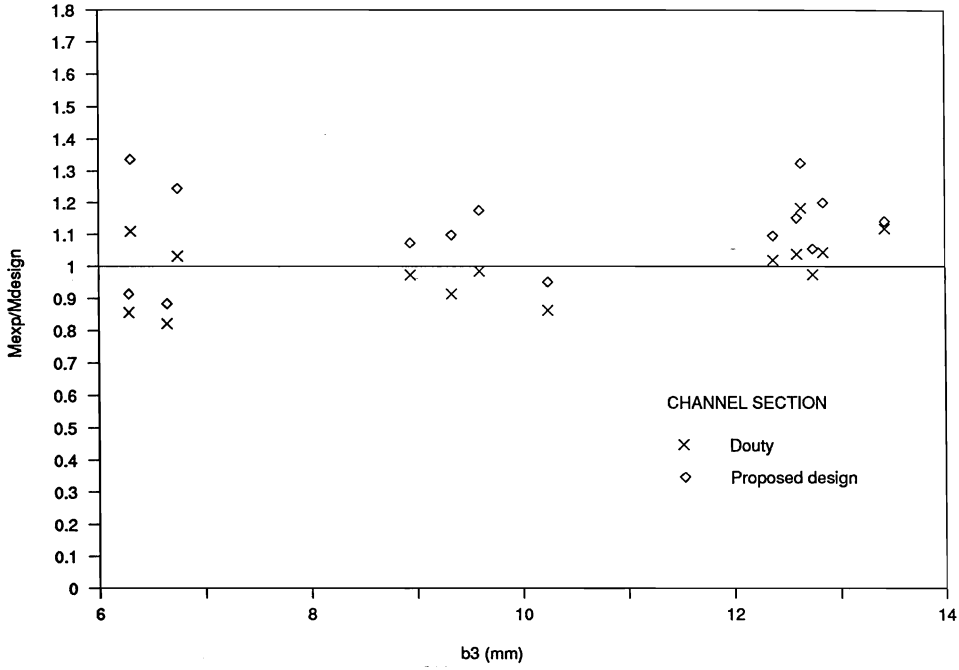

Figure 29

Top-Hat Section

spec.no	b3 (mm)	l_y (mm)	A (mm)	M_{exp} (kN.mm)	M_D/M_{exp}	M_{pd}/M_{exp}
AT2	8.04	660.4	76.2	Crush	N.A.	N.A.
AT3	10.77	609.6	101.6	387.13	1.104	1.05
AT4	13.8	609.6	101.6	440.8	1.162	1.119
AT5	16.98	660.4	76.2	Crush	N.A.	N.A.
AT6	20.36	609.6	101.6	453.50	1.449	1.087
AT7	23.43	609.6	101.6	526.7	1.39	0.964
AT8	26.61	609.6	101.6	548.2	1.463	0.947
AT10	7.34	584.2	127	352.49	1.011	0.960
AT11	10.72	584.2	127	426.66	1.156	1.099
AT12	13.1	584.2	127	476.82	1.193	1.161
AT13	17.07	584.2	127	512.14	1.302	1.075
AT14	20.05	638.2	101.6	Touching	N.A.	N.A.
AT15	22.33	584.2	127	526.26	1.511	1.066
AT16	26.89	584.2	127	614.56	1.506	0.965
AT18	7.74	533.4	152.4	495.89	0.982	0.892
AT19	10.62	533.4	152.4	695.09	0.884	0.815
AT20	13.89	533.4	152.4	784.1	0.928	0.844
AT21	16.77	533.4	152.4	767.14	1.073	0.878
AT22	19.84	533.4	152.4	760.78	1.234	0.923
AT23	22.82	533.4	152.4	737.47	1.317	0.900
AT24	26	533.4	152.4	938.79	1.209	0.781

Channel Section

spec.no	b3 (mm)	l_y (mm)	A (mm)	M_{exp} (kN.mm)	M_D/M_{exp}	M_{pd}/M_{exp}
AC3	6.47	661	76.2	188.2	1.189	1.217
AC4	6.3	610.2	76.2	175	1.246	1.268
AC5	9.59	661	76.2	211.92	1.596	1.548
AC6	9.74	661	76.2	213.61	1.590	1.546
AC7	13.42	661	76.2	491.65	0.893	0.875
AC8	12.74	483.2	165.1	409.6	1.026	0.947
AC11	6.28	483.2	165.1	257.2	1.167	1.094
AC12	6.64	483.2	165.1	293.87	1.217	1.132
AC13	8.94	483.2	165.1	422.42	1.027	0.932
AC14	10.24	483.2	165.1	443.74	1.159	1.051
AC15	12.37	483.2	180.34	629.94	0.981	0.911
AC16	12.59	483.2	180.34	560.123	0.963	0.867
AC19	6.3	483.2	165.1	394.2	0.901	0.748
AC20	6.74	483.2	165.1	378.35	0.969	0.803
AC21	9.59	483.2	180.34	465.43	1.016	0.850
AC22	9.33	483.2	171.45	427.23	1.094	0.911
AC23	12.63	483.2	180.34	730.25	0.844	0.753
AC24	12.84	483.2	180.34	597.84	0.957	0.832

TABLE 5 COMPARISON OF EXPERIMENT ULTIMATE MOMENTS WITH DESIGN RULES

Figure (30) shows that for test series A specimens (l_p=483 to 661mm), the governing failure mode will be the symmetrical buckling mode. For test series B specimens (L=2m), the governing failure mode will be the lateral-torsional buckling mode. These two modes of failure are the same as those observed during the experiments. This figure also shows that Douty's method only applies to the case of small lip widths. For large lip widths, even considering failure due to inelastic buckling using Douty's method still lead to overestimation of the actual ultimate moment.

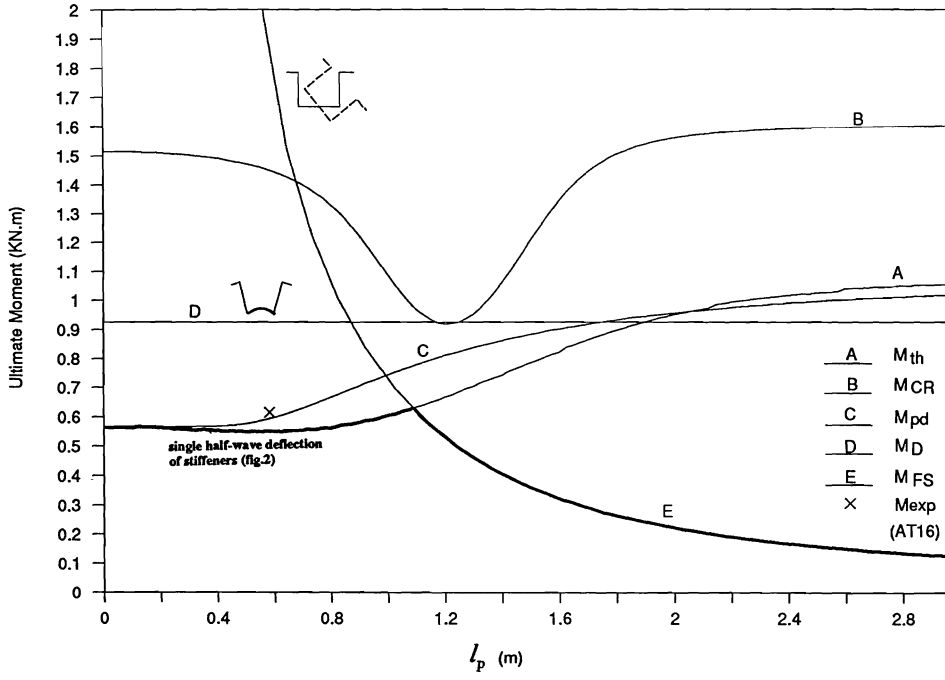

Figure 30

Table (6) shows the comparisons of experimental ultimate moments with those determined theoretically, according to B.S. 5950: Part 5 and design rules proposed by Rhodes [6] for test series A, unlipped specimens. The predicted ultimate moments based on British Standard are very conservative, compared to the experiment results. This is because the post-buckling strength is not allowed to be fully utilised in the British Standard. The theoretical critical moments shown in this figure are in better agreement with the experiment results. The ultimate moments predicted based on Rhodes's design rules [6] also agree well with the experimental results.

Spec.no	M_{BS} (kN.mm)	M_{BS}/Mexp	M_R (kN.mm)	M_R/Mexp	M_{CR} (kN.mm)	M_{CR}/Mexp
AC1	64.41	0.475	94.4	0.7	96.89	0.714
AC2	64.93	0.476	95.05	0.697	97.92	0.718
AC9	107.93	0.577	153.96	0.824	172.96	0.925
AC10	123.28	0.712	171.22	0.989	206.02	1.190
AC17	147.71	0.644	190.82	0.834	269.85	1.176
AC18	151.21	0.655	194.74	0.843	277.31	1.201
AT1	81.62	0.571	118.08	0.825	126.68	0.885
AT9	104.67	0.554	148.86	0.788	168.42	0.891
AT17	167.06	0.674	215.15	0.868	272.07	1.097

M_{BS}= Predicted ultimate moment based on B.S.5950:part 5
M_{CR}= Theoretical critical moment (e=0 case)
M_R= Predicted ultimate moment based on Rhodes [6] design rules

TABLE 6 COMPARISON OF ULTIMATE MOMENTS FOR UNLIPPED SPECIMENS

9. CONCLUDING REMARKS

A type of buckling behaviour is reported for short beams of edge stiffened cross section bent in such a way that the edge stiffeners are in compression. This buckling behaviour is characterized by the tendency of the compression stiffeners to buckle in the lateral direction accompanied by out-of-plane bending of the web.

From the investigation, it was found that in-plane bending of the lips is very much dependant on the beam length, and is more likely to occur in short beams.

All in all, it can be concluded that depending on the length; for short beams the governing failure mode will be the symmetrical buckling mode. When the lip width is small or inadequate ($b_3/b_2<0.25$), the beam will tend to buckle into more than one half-wave length. For large or adequate ($b_3/b_2\geq0.25$) lip width, the single half-wave buckling mode will be the governing failure mode.

It should be noted that this type of buckling is not a bifurcation buckling, but the lateral deflections of the lips grow from the start of loading. Even in the case of very large lips, the lip capacity is substantially reduced for short beams loaded in this way. This may have significant implications for continuous beams which undergo such loading over a short length of span or in the region of intermediate supports.

In general, the experimental results obtained indicate that the theoretical analysis fairly accurately describes the behaviour of the beams investigated. Design procedures were formulated based on the theoretical analysis with a limiting plate width to thickness ratio of 60. The design procedures proposed can predict with reasonable accuracy, the ultimate moment of the beam sections. This reflects the rationality of the design procedures.

In designing such lipped channel beams, with edge stiffened webs bent in such a way that the unbraced stiffeners are in compression, the lowest of the two moment capacities calculated from the proposed design rules and the lateral-torsional buckling load from another analysis, should be used.

APPENDIX I-REFERENCES

1 DOUTY, R. T.
"A Design Approach to The Strength of Laterally Unbraced Compression Flanges"
Engineering Experimental Station Bulletin, No.37, Cornell Univ. 1962.

2 YU, WEI-WEN
"Cold-Formed Steel Structures"
McGraw-Hill, New York. 1973.

3 RHODES, J.
"A Simple MicroComputer Finite Strip Analysis"
Dynamics of Structures, Proc. of The Session At Structures Congress '87. ASCE, ISBN 0-87262-615-6, pp.276-291, 1987.

4 SEAH, L.K.
"Buckling Behaviour of Edge Stiffeners In Thin-Walled Structures"
Ph.D Thesis, University of Strathclyde, 1989.

5 BRITISH STANDARDS INSTITUTION
"B.S. 5950:PART 5. 1987, Code of Practice For Design of Cold Formed Sections"
BSI, London. 1987.

6 RHODES, J.
"Research into the Mechanical Behaviour of Cold-Formed Sections and Drafting of Design Rules"
ECSC Contract No. 7210/SA/608, Univ. of Strathclyde, April 1987.

7 RHODES, J.
"Effective Widths in Plate Buckling"
Development In Thin-Walled Structures, edited by J. Rhodes and A. C. Walker, Applied Science, London, 1982.

8 RHODES, J.
"The Non-Linear Behaviour of Thin-Walled Beams Subjected to Pure Moment Loading"
Ph.D Thesis, University of Strathclyde, 1969.

9 WINTER, G.
"Stress Distribution In and Equivalent Width of Flanges of Wide, Thin-Wall Steel Beams"
NACA, Tech. note No. 784, 1940

APPENDIX II-NUMERICAL CONSTANTS

$$B_1 = \frac{b_1}{2} + \frac{b_1}{8}\left(\frac{\pi}{b_1}\right)^4 \frac{l_p^4}{180} + \left(\frac{\pi}{b_1}\right)^2 \left[\frac{2}{3}(b_2^3 + b_3^3) + \frac{l_p^2}{3}(1-\upsilon)\left(b_2 + b_3 + \frac{b_1}{4}\right)\right]$$

$$B_2 = \frac{4b_1}{\pi} - 2\left(\frac{\pi}{b_1}\right) b_3^2$$

$$B_3 = b_1\bar{y}^2 + 2b_2\bar{y}^2\left(1 - \frac{b_2}{\bar{y}} + \frac{b_2^2}{3\bar{y}^2}\right) + 2b_3(\bar{y} - b_2^2)^2$$

$$B_4 = b_3^4\left(\frac{\pi b_2}{b_1 A_T}\right)^2\left(\frac{2}{3}\frac{A_T^2}{b_3} - A_T\right)$$

$$B_5 = b_3^2\frac{\pi b_2}{b_1}(\bar{y} - b_2)$$

$$B_6 = \frac{3b_1}{8} - \frac{1}{A_T}\left[\frac{b_1}{2} + \left(\frac{\pi}{b_1}\right)^2\left(\frac{2}{3}(b_2^3 + b_3^3) + 2b_3 b_2^2\right)\right]^2 + (\frac{\pi}{b_1})^4\left(\frac{2}{5}(b_2^5 + b_3^5) + 2b_2^4 b_3 + \frac{4}{3}b_2^2 b_3^3\right)$$

$$B_7 = \frac{b_2}{12A_T}\left(\left(\frac{\pi}{b_1}\right)^2 [2b_2^4 + 3b_1 b_2^3 + 4b_1 b_3^3 + 4b_2 b_3^3 + 10b_2^3 b_3 + 12b_1 b_2^2 b_3] - 3b_1[b_2 + 2b_3]\right)$$

$$B_8 = \frac{\pi}{12}\frac{b_2 b_3^2}{A_T}\left(3 - \left(\frac{\pi}{b_1}\right)^2\left[6b_2^2 + 8\frac{b_2^3}{b_1} + 3b_3^2 + 2\frac{b_3^3}{b_1} + 6\frac{b_2 b_3^2}{b_1}\right]\right)$$

If 'e' is zero, then B_1 and B_2 becomes:

$$B'_1 = \frac{b_1}{2} + \frac{b_1}{8}\left(\frac{\pi}{b_1}\right)^4 \frac{l_p^4}{30} + \left(\frac{\pi}{b_1}\right)^2\left(\frac{2}{3}(b_2^3 + b_3^3) + l_p^2\left[\frac{b_1}{12} + \frac{1^2}{3}(1-\upsilon)(b_2 + b_3)\right]\right)$$

$$B'_2 = \frac{4b_1}{\pi} + 2\left(\frac{\pi}{b_1}\right)\left(\upsilon\frac{l_p^2}{6} - b_3^2\right)$$

APPENDIX III-NOTATION

A	distance between support and loading knife edges
C	curvature coefficient due to bending
C_{cR}	critical curvature
d	curvature coefficient due to lateral displacement of the lips
D	plate flexural rigidity $Et^3/[12(1-\upsilon^2)]$
e	arbitrary deflection constant
E	Young's modulus of Elasticity
h_L	lip to web width ratio
h_t	web width to thickness ratio
l_p, L_p	length of beam subjected to pure moment
l_s	length between the two supports.
L_b	length to web width ratio
L	Total length of specimen
M_{CR}	theoretical critical moment
M_D	critical moment determined using Douty's [1] method
M_{exp}	experimental ultimate moment
M_{FS}	critical moment determined using Finite Strip program by Rhodes [3]
M_{inad}	moment capacity of inadequately stiffened beam section
M_{pd}	ultimate moment based on proposed design procedures
M_s	moment capacity of adequately stiffened beam section
M_{th}	theoretical moment assuming buckling into single half-wave
M_u	moment capacity of unstiffened beam section
$\overline{M}_{ult}$	non-dimensional ultimate moment, $M_{ult}/(\sigma_y t b_2^2)$
$\overline{M}$	non-dimensional moment, $M/(\sigma_y t b_2^2)$
R	web to flange width ratio
t	thickness of plate
V_{BT}	total strain energy due to bending and twisting of plate system
V_i	in-plane deflected form of plate component (i=1, 2, 3)
V_{MT}	total membrane energy
W_i	out-of-plane deflected form of plate component (i=1, 2, 3)
Z_c	effective compression section modulus
Z_{inad}	effective compression section modulus of inadequately stiffened beam section
Z_s	effective compression section modulus of adequately stiffened beam section
Z_u	effective compression section modulus of unstiffened beam section
σ_p	stress distribution on the plate
σ_i	stress distribution on the stiffeners or plate component (i=1,2,3)
σ_{Ai}	stress distribution on plate component due to bending (i=1,2,3)
σ_B	stress due to the lateral displacement of lip
σ_{CR}	critical buckling stress
σ_y	yield stress of material
δ_c	centre deflection of beam